

# Exploring Jet-Hadron correlations at the LHC with ALICE

**Joel Mazer**

Department of Physics, University of Tennessee, Knoxville, Tennessee 37996-1200, USA

E-mail: [joel.mazer@cern.ch](mailto:joel.mazer@cern.ch)

**Abstract.** In relativistic heavy ion collisions at the Large Hadron Collider (LHC), the conditions are met to produce the hot and dense, strongly interacting medium known as the Quark Gluon Plasma (QGP). The QGP, a state of matter created shortly after the Big Bang, is a phase where the deconfinement of quarks and gluons is hypothesized. Jets, the collimated sprays of hadrons from fragmenting partons, are a key probe of the medium. The experimental methods used for jet measurements at ALICE to remove, reduce, and correct for the underlying background event will be presented. In pp collisions, jet production is well understood within the framework of perturbative QCD and acts as a rigorous baseline measurement for jet quenching measurements. By comparing to heavy ion collision systems, we can study the suppression of the number of jets seen and study the modification of the  $p_T$  or angular distributions of jet fragments. Azimuthal angular correlations of charged hadrons with respect to the axis of a full (charged + neutral) reconstructed (trigger) jet in Pb–Pb and pp collisions at  $\sqrt{s_{NN}} = 2.76$  TeV in ALICE will be presented here. Newly developed combinatoric background subtraction methods and their improvement compared to prior techniques will be discussed.

## 1. Introduction

In heavy ion collisions, a hot and dense QCD medium is formed [1, 2]. Jets are an ideal probe because the hard-scattered partons which produce them are created very early in the collision, prior to formation of the medium, or Quark Gluon Plasma (QGP). Partons resulting from the hard scatterings in heavy ion collisions are modified in the presence of a medium through induced gluon radiation and collisional energy loss [3, 4]. This modification was observed at both RHIC and LHC energies via the suppression of high-momentum particles [5–8]. Jets can also be used as a probe by studying the suppression of the number of jets in Pb–Pb collisions compared to baseline measurements in pp or pPb collisions. A similar suppression can also be observed for high  $p_T$  di-hadrons correlations [9–12].

Measurements of jets in pp collisions offer a reference for comparing the medium induced jet modifications in heavy ion collisions. The production cross section of jets in pp collisions are calculable using perturbative Quantum Chromodynamics (pQCD). Jet measurements in pp collisions also allow for a quantitative understanding of the impact of hadronization on reconstructed jets [13].

## 2. Experimental setup

In ALICE, jets are reconstructed using charged particles measured with the central tracking system and clusters measured in the Electromagnetic Calorimeter (EMCal). Tracks from charged



particles are reconstructed using information from the Time Projection Chamber (TPC) and Inner Tracking System (ITS). The TPC is the main tracking detector of the central barrel and provides particle identification (PID) and charged particle momentum measurements [14]. The ITS is a six-layer silicon detector with that provides a precise measurement of the primary vertex location. The two inner layers of the ITS, known as the Silicon Pixel Detector (SPD), are also used for selecting high quality tracks coming from the primary collision [15]. Tracks reconstructed for jet analyses come from mid-rapidity ( $|\eta_{lab}| < 0.9$ ) and cover the full range in azimuth. The tracking detectors measure particles down to 0.15 GeV/ $c$  in transverse momentum ( $p_T$ ). The EMCal is a Pb-scintillator sampling calorimeter which has an acceptance of  $|\eta_{lab}| < 0.7$  and  $|\Delta\phi| = 107^\circ$  [16]. For a complete description of the ALICE experiment detector system see [17].

### 3. Jet Reconstruction

There is no unique definition of a jet. Experimentally, we measure the jet through particles which are produced in the fragmentation of quarks and gluons and seen as tracks and clusters. These fragments are expected to reflect the kinematics and topology of the originating partons. We need a general definition to apply to both theory and experimental calculations which, consists of a jet-finding algorithm, its parameters, and a recombination scheme. ALICE uses the  $k_T$  and anti- $k_T$  jet-finding algorithms from the FastJet package [18]. A jet-finding algorithm defines how tracks and clusters in the detector (experiment) or partons (theory) are grouped into jets. For the  $k_T$  and anti- $k_T$  methods, the algorithms group nearby objects together pair-wise until all particles are clustered into jet candidates. In ALICE, we use the anti- $k_T$  algorithm for our jet signal, which merges the highest  $p_T$  particles first. It has the advantage of creating a circular shape around the jet constituents, defined by the jet resolution parameter  $R$ , which is given by  $R = \sqrt{(\Delta\eta)^2 + (\Delta\phi)^2}$ .  $R$  is used to set the maximum distance in pseudorapidity  $\eta$  and azimuthal angle  $\phi$  that constituent particles can be clustered together when reconstructing a jet [18]. For calculating the background energy from the underlying event uncorrelated to the hard scattering, we use the  $k_T$  algorithm which is not bound to a circular structure and begins by clustering the lowest  $p_T$  particles first. In ALICE, the boost-invariant sequential recombination scheme is used [18].

By studying fully reconstructed jets, several variables associated with jet reconstruction can be adjusted allowing for them to serve as very versatile triggers [19]. By selecting high  $p_T$  leading jets, it is expected that the jet production points are biased towards the surface of the interaction region. This is known as surface biasing and the initial energy of the parton on the opposing side can be approximated more accurately [19]. In principle, by adjusting the surface bias of the trigger jet through various cuts [19], we can adjust the pathlength traversed through the medium of the opposing jet and perform true jet tomography [20]. Applying a constituent cut or imposing a leading track requirement on the reconstructed jet enhances the surface bias by forcing the jet to be harder and rejects combinatorial jets from the measurement. Combinatorial jets are reconstructed jets which do not originate from a hard process. These cuts don't affect the opposing jet being studied. [19]

## 4. Spectra results

### 4.1. Data sample

The data used for the spectra analyses was collected in 2011 by ALICE during the 2.76 TeV pp and 2.76 TeV Pb–Pb collision runs. The pp collisions include two different triggers to perform the spectra measurement. A combination of a minimum bias (MB) trigger and an EMCal trigger requiring a single shower with  $E_T > 3$  GeV/ $c$  was used in order to allow for statistics to be collected over a wider  $p_T$  range of 20 to 125 GeV/ $c$  [13, 21, 22].

#### 4.2. pp collisions

In order to study the properties of the QCD medium generated in Pb–Pb collisions at LHC energies, a reference collision system is needed. In pp collisions, a medium is not expected to exist. Jet measurements performed in pp collisions serve as a baseline reference when interpreting the Pb–Pb collision results. These measured jets are corrected bin-by-bin in  $p_T$  back to the particle level [21]. Additional analysis details can be found in [21]. Figure 1 shows the inclusive differential jet cross section with  $R = 0.2$  at  $\sqrt{s} = 2.76$  TeV. We compare our measurement to various Next-to-Leading-Order (NLO) pQCD calculations [23,24], with and without the effects of hadronization [25] and at parton level. A good agreement to NLO calculations can be seen when including hadronization. This shows that we have a very good understanding of jet production in collisions where a medium is not produced.

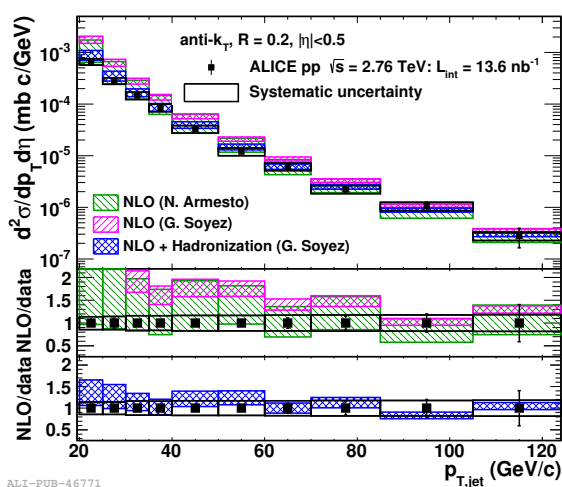


**Figure 1.** The inclusive differential  $R = 0.2$  full jet cross section in pp collisions at  $\sqrt{s} = 2.76$  TeV. A comparison of the experimental calculation is shown to NLO pQCD calculations both with and without the effects of hadronization. The systematic uncertainty is designated by the box around the data points. [21]

#### 4.3. Pb–Pb collisions

The jets produced in heavy ion collisions sit on top of a large amount of soft ( $p_T < 2.0$  GeV/c) background. The variable most often used to quantify this background is  $\rho$ , which refers to the underlying event background energy density. The procedure for obtaining  $\rho$  requires clustering all charged tracks in the event into groups using the  $k_T$  jet-finding algorithm provided by FastJet [18]. The two leading jets in the event are removed and the underlying event background density is expressed as the median of the summed  $p_T$  per area ( $A_{k_T jet}$ ) of the remaining  $k_T$  clusters and is given by Eq. 1.

$$\rho_{ch} = \text{median} \left( p_{T, k_T jet}^{ch} / A_{k_T jet} \right) \quad (1)$$

In order to reduce the bias due on jet fragmentation, tracks with  $p_T^{min} > 0.15$  GeV/c are used in this analysis. It is shown in [26] that the background density depends on event multiplicity and that the spread of  $\rho$  in a given centrality bin is considerable. This serves as motivation for an event-by-event background subtraction performed on a jet-by-jet basis.

When reconstructing full jets, the neutral energy component is compensated for by scaling the charged background density distribution by the EMCAL scale factor,  $\rho_{scaled} = \rho_{ch} \times s_{EMC}$ , where  $s_{EMC}$  is defined by Eq. 2 and parametrized as a function of multiplicity.

$$s_{EMC} = \frac{\left( \sum p_T^{track} + \sum E_T^{cluster} \right)}{\sum p_T^{track}} \quad (2)$$

From the results of [8, 26], it can be seen that for the 10% most central events, the scaled background density amounts to roughly 200 GeV/c per unit area. The average background for a full jet in a central collision with  $R = 0.2$  is 25 GeV/c. This is subtracted from our reconstructed jet  $p_T$  via Eq. 3. For additional analysis details, see [8, 26].

$$p_{T,jet}^{unc} = p_{T,jet}^{rec} - \rho_{scaled} A_{jet} \quad (3)$$

Figure 2 shows the inclusive jet yields per event for  $R = 0.2$  full jets at  $\sqrt{s_{NN}} = 2.76$  TeV in both the 0-10% and 10-30% centrality classes compared to the measurement at the same  $\sqrt{s}$  in pp collisions. A leading charged jet constituent with  $p_T > 5$  GeV/c is required to reduce the combinatorial background and improve unfolding stability. To compare the two datasets, the Pb-Pb results are divided by the number of binary collisions,  $N_{coll}$ , calculated in a Monte Carlo Glauber model [27] which assumes independent binary nucleon-nucleon collisions.

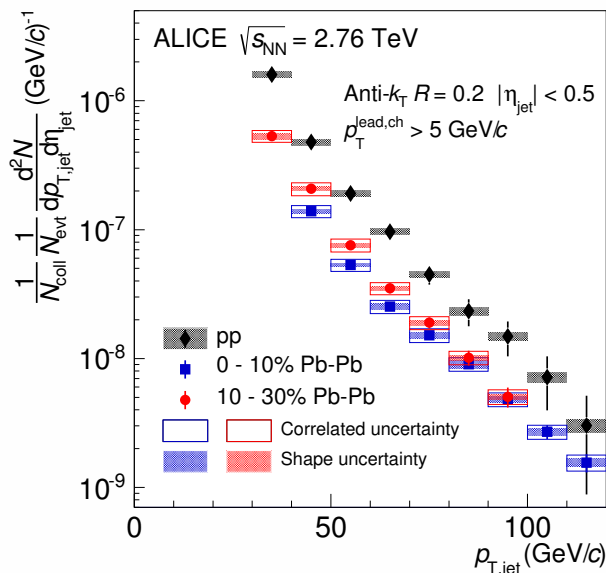


**Figure 2.** The inclusive spectra for  $R = 0.2$  full jets in Pb-Pb collisions at  $\sqrt{s_{NN}} = 2.76$  TeV reconstructed with a leading charged track bias of 5 GeV/c. For comparison, 0-10%, 0-30% are plotted with the results from pp collisions and normalized by  $N_{coll}$ . All three are normalized per event. [8]

The nuclear modification factor,  $R_{AA}$ , is defined by Eq. 4 and is the ratio of the Pb-Pb per-event yield divided by the pp cross section multiplied by  $T_{AA} = N_{coll}/\sigma_{pp}^{inel}$  [27].

$$R_{AA} = \frac{1}{T_{AA}} \frac{d^2 N_{jets}}{dp_T d\eta} \frac{d^2 \sigma}{dp_T d\eta} \quad (4)$$

A value greater (less) than 1.0 indicates an enhancement (suppression) in Pb-Pb relative to pp collisional system. The  $R_{AA}$  for  $R = 0.2$  full jets is shown in Fig. 3 for both 0-10% and 10-30% central events. Jet suppression is seen to be centrality dependent, and within both the statistical and systematic uncertainties the two measurements are independent of  $p_T^{jet}$  [8, 13]. The largest suppression occurs for the 0-10% most central events with an  $R_{AA} = 0.28 \pm 0.04$  [8]. The suppression fairly agrees within error to both YaJEM [28] and JEWEL [29], which are different models for energy loss in the medium [8].

## 5. Correlation results

Correlation measurements are powerful tools which can be used to probe the jet-medium interactions in AA collisions, provide additional constraints on energy loss models and thereby

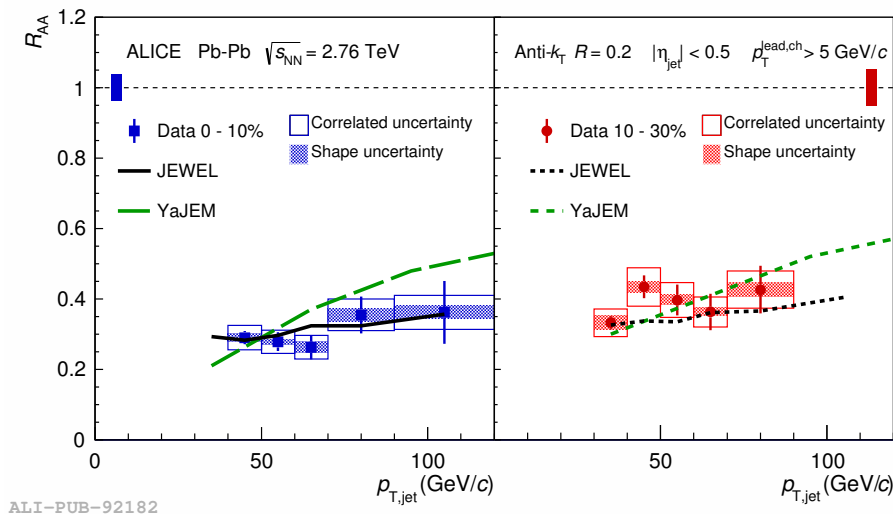


**Figure 3.** The nuclear modification factor,  $R_{AA}$ , for  $R = 0.2$  full jets in 0-10% (left) and 10-30% (right) central events. Also shown are calculations from YaJEM [28] and JEWEL [29]. [8]

provide us with a better understanding of the properties of the QGP [19]. The jet-hadron correlation function is defined in Eq. 5 [19] as the number of same event pairs to the number of mixed event pairs.

$$\frac{1}{N_{trig}} \frac{dN}{d\Delta\varphi} = \frac{1}{\epsilon N_{trig}} \frac{\frac{dN_{pairs}^{same}}{d\Delta\varphi}}{\frac{dN_{pairs}^{mixed}}{d\Delta\varphi}} \quad (5)$$

Where  $N_{trig}$  corresponds to the number of trigger jets and  $\eta$  is the efficiency of the associated particles. The mixed event pair distribution, which corrects for the detector acceptance effects, is normalized such that the  $(\Delta\varphi = 0, \Delta\eta = 0)$  bin is 1.0. The resulting distribution is then projected to show the angular correlations between the jet and the associated particles given by  $\Delta\varphi = \varphi_{jet} - \varphi_{assoc}$ . When studying the correlations from baseline pp collisions, a peak is seen on the near side at  $\Delta\varphi = 0$  and on away side at  $\Delta\varphi = \pi$  [19]. The near-side is due to the associated particles of the trigger jet that defines the  $\Delta\varphi = 0$  position. The away-side is then due to the particles associated with the opposite jet created from the initial hard scattering.

At RHIC, the STAR collaboration has studied jet-hadron correlations in Au+Au at 200 GeV [30]. They calculated the away-side energy balance function,  $D_{AA}$ , which measures the  $p_T$  difference of the associated particle yield between AuAu and pp collisions for a given  $p_T^{assoc}$  bin. The results show that the suppression of high- $p_T$  hadron yield on the away side is in large part balanced by an enhancement at low- $p_T$ . They also showed an away-side jet width measurement which suggests there is jet broadening to large angles at low- $p_T$  when compared to pp collisions, but the significance is limited due to large uncertainties of the jet  $v_n$  used in the determination of the heavy ion background. These results imply that most modifications to jets occur at low hadron  $p_T$ . At LHC, we can study the effect at higher  $\sqrt{s_{NN}}$  and access higher parton energies. In ALICE, our particle identification and reconstruction with the ALICE Time-Of-Flight (TOF) detector and the TPC works best at these lower transverse momenta and therefore allows us to measure identified particles in jets.

### 5.1. Data sample

The data used for the correlations analyses was collected in 2011 by ALICE during the 2.76 TeV pp and 2.76 TeV Pb–Pb collision runs. The pp collisions includes events that fired the trigger used by the ALICE electromagnetic calorimeter (EMCal), which requires a shower containing more than 3 GeV of energy for acceptance [19]. This allows for enhanced statistics provided by the resulting data sample.

### 5.2. pp correlations

Figure 4 shows the jet-hadron measurement for pp collisions at  $\sqrt{s} = 2.76$  TeV [19]. The  $R = 0.4$  trigger jets are 20–60 GeV/c with constituent particles  $> 3$  GeV/c and have a 6 GeV/c leading track bias. The correlations are shown for associated particles in three bins: [0.5, 1.0], [1.0, 2.0], and [2.0, 3.0] GeV/c. The background subtraction of the underlying event is estimated by using a flat pedestal since the jet-hadron correlations in the  $\Delta\eta$  range shown in Fig. 4 ( $|\Delta\eta| < 0.4$ ) were rather flat. The uncertainty from this subtraction is shown as the grey band about 0 [19]. The efficiency correction caused an overall uncertainty on the normalization of the correlation function of 7% [19]. We see a general decrease in the jet widths as we increase the associated track momentum and observe it to be less significant on the away-side [19]. These results agree with expectations [19] and serve as our baseline for heavy ion measurements.

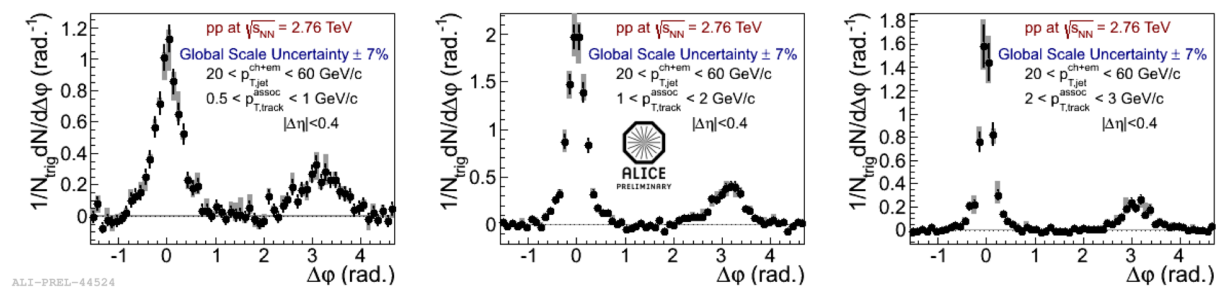


**Figure 4.** The pp baseline jet-hadron correlations measurement of ALICE for 3 associated momentum bins. The  $\Delta\phi$  distributions are shown for 20–60 GeV/c jets reconstructed using the anti- $k_T$  algorithm. These reconstructed jets have a resolution parameter of  $R = 0.4$ , constituent particles  $> 3$  GeV/c, and require a track bias of  $p_T > 6$  GeV/c. The uncertainty from the pedestal background subtraction is shown as the grey band. [19]

### 5.3. Pb–Pb correlations

In heavy ion collisions our correlation function now takes on an additional term and is expressed by Eq. 6 [19].

$$\frac{1}{N_{\text{trig}}} \frac{dN}{d\Delta\phi} = \frac{1}{\epsilon N_{\text{trig}}} \frac{dN_{\text{pairs}}^{\text{same}}}{d\Delta\phi} - b_0 \left( 1 + \sum v_n^{\text{trig}} v_n^{\text{assoc}} \cos(n\Delta\phi) \right) \quad (6)$$

The second term accounts for the underlying event of heavy ion collisions which is now modulated by hydrodynamical flow. To subtract off this background, the knowledge or calculation of the Fourier coefficients ( $v_n$  terms) from the trigger jet and associated particles are needed. A first look towards jet-hadron correlations without the background subtraction or efficiency correction is seen in Fig. 5 for Pb–Pb collisions. It is for  $R = 0.4$  jets of 20–60 GeV/c,

constituents with  $p_T > 3 \text{ GeV}/c$ , and associated particles of  $2 - 3 \text{ GeV}/c$ . There is a near-side peak observed, but not much can be concluded until the background is understood and subtracted.

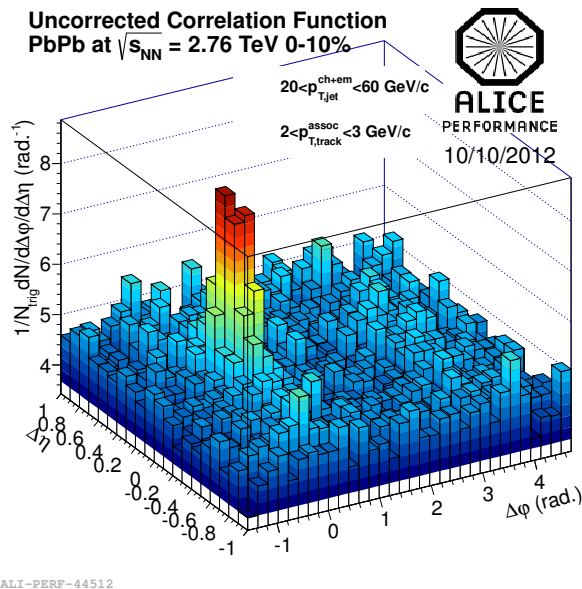


**Figure 5.** The uncorrected correlation function for full jets in Pb–Pb collisions at  $\sqrt{s_{NN}} = 2.76 \text{ TeV}$  for the 0-10% most central events. These results have yet to have an efficiency correction applied or the flow background removed. [19]

## 6. Background subtraction

In order to analyze the jet-hadron correlation signal in Pb–Pb collisions, it becomes necessary to understand and subtract the large combinatoric background. In addition to the large background produced, collective flow effects contribute to the bulk particle production in a similar way to that of correlations strictly due to jet production and this dominates at low momenta. With the aim of improving the constraints of prior studies of the combinatoric background, various background methods were developed in [31]. Two key methods were the near-side fit (NSF) and the reaction plane fit (RPF). The NSF method works under the assumption that the signal is negligible in the large  $\Delta\eta$  and small  $\Delta\phi$  region. This background dominated region is projected for  $1.0 < |\Delta\phi| < 1.4$  and Eq. 7 is fit up to  $n=4$  for  $|\Delta\phi| < \pi/2$  and extrapolated over the full range of  $\Delta\phi$ .

$$\frac{dN^{pairs}}{\pi\Delta\phi} = B(1 + \sum_{n=1} 2v_n^{trigger} v_n^{assoc} \cos(n\Delta\phi)) \quad (7)$$

The NSF method does not require independent measurements of  $v_n$  and is able to fit the background and therefore extract the signal with less bias and smaller errors than the ZYAM method [31]. When the trigger is restricted relative to the reaction plane, both the background level and effective  $v_n$  are modified [32]. The RPF method is an extension of the NSF method which uses the reaction plane dependence of the correlation function to determine the background to higher precision. It was shown by [31] that the RPF works very effectively while using fewer assumptions and has smaller errors than other background methods. For more method details, see [31].

## 7. Summary and Outlook

The jet spectra and jet-hadron correlations measurements in ALICE were shown for pp collisions at  $\sqrt{s} = 2.76 \text{ TeV}$ . They establish baseline measurements needed for understanding modification

to jets in the presence of a medium. The Pb–Pb spectra of the same collisional energy was shown and compared to the pp collision baseline in the  $R_{AA}$  measurement. It was seen that jets from Pb–Pb collisions are suppressed in a centrality dependent way, but nearly independent across  $p_T^{jet}$  bins to within both systematic and statistical uncertainties. This helps establish jets as a very critical probe toward understanding the QGP. We then gave an early look at the jet-hadron correlations in Pb–Pb collisions. Higher statistics and improved background subtraction techniques allow higher precision measurements of jet widths and yields. Jet-hadron correlations relative to the event plane are in progress.

## References

- [1] Adcox K *et al.* (PHENIX) 2005 *Nucl. Phys.* **A757** 184–283 (*Preprint nucl-ex/0410003*)
- [2] Adams J *et al.* (STAR) 2005 *Nucl. Phys.* **A757** 102–183 (*Preprint nucl-ex/0501009*)
- [3] Qin G Y, Ruppert J, Gale C, Jeon S, Moore G D and Mustafa M G 2008 *Phys. Rev. Lett.* **100** 072301 (*Preprint 0710.0605*)
- [4] Zakharov B G 2007 *JETP Lett.* **86** 444–450 (*Preprint 0708.0816*)
- [5] Adare A *et al.* (PHENIX) 2008 *Phys.Rev.* **C77** 011901 (*Preprint 0705.3238*)
- [6] Adams J *et al.* (STAR) 2003 *Phys. Rev. Lett.* **91** 172302 (*Preprint nucl-ex/0305015*)
- [7] Adare A *et al.* (PHENIX) 2011 *Phys.Rev.* **C84** 024904 (*Preprint 1010.1521*)
- [8] Adam J *et al.* (ALICE) 2015 *Phys. Lett.* **B746** 1–14 (*Preprint 1502.01689*)
- [9] Adams J *et al.* (STAR Collaboration) 2005 *Phys. Rev. Lett.* **95**(15) 152301
- [10] Abelev B I *et al.* (STAR Collaboration) 2009 *Phys. Rev. C* **80**(6) 064912
- [11] Agakishiev G *et al.* (STAR Collaboration) 2012 *Phys. Rev. C* **85**(1) 014903
- [12] Aggarwal M M *et al.* (STAR Collaboration) 2010 *Phys. Rev. C* **82**(2) 024912
- [13] Reed R and Collaboration A 2015 *Journal of Physics: Conference Series* **636** 012010
- [14] Alme J *et al.* 2010 *Nuclear Instruments and Methods in Physics Research Section A: Accelerators, Spectrometers, Detectors and Associated Equipment* **622** 316 – 367 ISSN 0168-9002
- [15] Abelev B *et al.* (ALICE) 2014 *J. Phys.* **G41** 087002
- [16] Abeysekara U *et al.* (ALICE EMCAL) 2010 (*Preprint 1008.0413*)
- [17] Abelev B B *et al.* (ALICE) 2014 *Int. J. Mod. Phys.* **A29** 1430044 (*Preprint 1402.4476*)
- [18] Cacciari M, Salam G P and Soyez G 2012 *Eur.Phys.J.* **C72** 1896 (*Preprint 1111.6097*)
- [19] Connors M 2013 *Journal of Physics: Conference Series* **446** 012009
- [20] Renk T 2013 *Phys. Rev.* **C87** 024905 (*Preprint 1210.1330*)
- [21] Abelev B *et al.* (ALICE) 2013 *Phys. Lett.* **B722** 262–272 (*Preprint 1301.3475*)
- [22] Ma R (ALICE) 2013 *Nucl. Phys.* **A910-911** 319–322 (*Preprint 1208.4537*)
- [23] Frixione S, Kunszt Z and Signer A 1996 *Nucl. Phys.* **B467** 399–442 (*Preprint hep-ph/9512328*)
- [24] Frixione S 1997 *Nucl. Phys.* **B507** 295–314 (*Preprint hep-ph/9706545*)
- [25] Cacciari M, Rojo J, Salam G P and Soyez G 2011 *Eur. Phys. J.* **C71** 1539 (*Preprint 1010.1759*)
- [26] Abelev B *et al.* (ALICE) 2012 *JHEP* **1203** 053 (*Preprint 1201.2423*)
- [27] Abelev B *et al.* (ALICE) 2013 *Phys. Rev.* **C88** 044909 (*Preprint 1301.4361*)
- [28] Renk T 2013 *Phys. Rev.* **C88** 014905 (*Preprint 1302.3710*)
- [29] Zapp K C 2014 *Phys. Lett.* **B735** 157–163 (*Preprint 1312.5536*)
- [30] Adamczyk L *et al.* (STAR) 2014 *Phys.Rev.Lett.* **112** 122301 (*Preprint 1302.6184*)
- [31] Sharma N, Mazer J, Stuart M and Natrass C 2016 *Phys. Rev.* **C93** 044915 (*Preprint 1509.04732*)
- [32] Bielcikova J, Esumi S, Filimonov K, Voloshin S and Wurm J 2004 *Phys.Rev.* **C69** 021901 (*Preprint nucl-ex/0311007*)